Journal of Solid State Chemistry 182 (2009) 836–840

Contents lists available at ScienceDirect

Journal of Solid State Chemistry

journal homepage: www.elsevier.com/locate/jssc

Synthesis and structural studies of lanthanide substituted bismuth–titanium pyrochlores

Jimmy Ting [a], Brendan J. Kennedy [a,*], Ray L. Withers [b], Maxim Avdeev [c]

[a] School of Chemistry, The University of Sydney, Sydney, NSW 2006, Australia
[b] Research School of Chemistry, Australian National University, Canberra, ACT 0200, Australia
[c] Bragg Institute, Australian Nuclear Science and Technology Organisation, Private Mail Bag 1, Menai, NSW 2234, Australia

ARTICLE INFO

Article history:
Received 28 October 2008
Received in revised form
16 December 2008
Accepted 31 December 2008
Available online 19 January 2009

Keywords:
Bismuth pyrochlore
Lanthanide substituted bismuth titanate
Crystal structure
Ferroelectric

ABSTRACT

The identity of the pyrochlore phase seen during the synthesis of ferroelectric $Bi_{4-x}Ln_xTi_3O_{12}$ Aurivillius oxides is shown to be $Bi_{2/3}Ln_{4/3}Ti_2O_7$. This pyrochlore is only stable for $Ln^{3+} = Sm^{3+}$ or smaller. For larger lanthanides the layered Aurivillius oxide is favoured. The presence of six-fold disorder, associated with the Bi $6s^2$ lone pair electrons, is believed to stabilise the unexpected stoichiometry of this oxide. Precise structures, obtained by Rietveld refinement from synchrotron X-ray diffraction data, of three examples Ln^{3+} = Eu, Ho and Yb are presented.

1. Introduction

Attempts to prepare single phase stoichiometric bismuth titanate pyrochlore, $Bi_2Ti_2O_7$, have utilised numerous routes including conventional solid state methods, sol–gel processing, co-precipitation and vapour deposition. Almost invariably the product is non-stoichiometric, i.e. $Bi_{1.83}Ti_2O_{6.75}$ as described by Radosavljevic et al. [1] and $Bi_{1.61}Zn_{0.18}Ti_{1.94}V_{0.06}O_{6.62}$ as reported by Khalenberg and Bohm [2] or contaminated with impurities such as $Bi_4Ti_3O_{12}$ [3,4]. The predisposition of bismuth titanate to yield non-stoichiometric structures can be rationalised by inspection of the pyrochlore structure.

The ideal $A_2B_2O_7$ pyrochlore structure is commonly described as a derivative of the fluorite structure where ordering of the A- and B-type cations over two sites results in a doubling of the unit cell to ca 10.5 Å [5]. In fact, the pyrochlore structure is better described as consisting of two interpenetrating networks, the first of composition A_2O' and the second of B_2O_6. The smaller B-type cation is within a B_2O_6 sublattice based on corner sharing BO_6 octahedra. The second sublattice is an A_2O' anti-cristobalite type, that occupies the hexagonal holes along the ⟨111⟩ direction of the B_2O_6 sublattice. Although the larger A-type cation is formally 8-coordinate, the two sublattices only weakly interact with the A–O distance (~2.5–2.7 Å) being considerably longer than the A–O′ distance, which is typically 2.1–2.2 Å. Energetically, the B_2O_6 network is the major contributor to the stability of the structure and vacancies within the A_2O' sublattice is commonplace.

The Ti_2O_6 sublattice in $Bi_2Ti_2O_7$ is expected to be relatively rigid with the Ti–O distance being close to the sum of the appropriate ionic radii (~1.95 Å) and the Ti–O–Ti angle being close to 135° [5]. Indeed Hector and Wiggin reported values of 1.964 Å and 137.5°, respectively, for $Bi_2Ti_2O_7$ at 2 K. [3]. The precise values of each of these parameters are given by the position of the oxygen atom on the 48*f* site at $(x\frac{33}{88})$. Movement of this oxygen together with the size of the lattice controls the size of the hexagonal holes along ⟨111⟩, and this is limited by electrostatic repulsion. Bond valence sums (BVS) suggest that the Bi^{3+} cation is too large to occupy the 16*c* sites at $(\frac{111}{222})$ in $Bi_2Ti_2O_7$ and alternate compositions such as $Bi_4Ti_3O_{12}$ are more thermodynamically stable.

Despite the limited stability of stoichiometric $Bi_2Ti_2O_7$, as described by Hector and Wiggin [3], a bismuth pyrochlore is commonly observed as an impurity in Bi–Ti Aurivillius oxides such as $Bi_4Ti_3O_{12}$ [6] and $Bi_{3.75}La_{0.25}Ti_3O_{12}$ [7]. The preference of the pyrochlore phase is very sensitive to *Ln* doping in $Bi_{4-x}Ln_xTi_3O_{12}$ and can have a significant impact on the ferroelectric properties of these technologically important oxides [8,9]. The above discussion presents a quandary—$Bi_4Ti_3O_{12}$ forms when attempting to produce the pyrochlore $Bi_2Ti_2O_7$ but a Bi–Ti pyrochlore often contaminates samples of the Aurivillius phases. Understanding this quandary together with the observation that non-stoichiometric bismuth pyrochlores such as $Bi_{1.5}Zn_{1.0}Nb_{1.5}O_7$ (BZN) [10,11] are promising dielectrics as a consequence of disorder of the Bi cation prompted us to examine some lanthanide doped bismuth titanates [12,13].

* Corresponding author. Fax: +61 2 9351 3329.
E-mail addresses: kennedyb@chem.usyd.edu.au, B.Kennedy@chem.usyd.edu.au (B.J. Kennedy).

0022-4596/$ - see front matter © 2009 Elsevier Inc. All rights reserved.
doi:10.1016/j.jssc.2008.12.030

The purpose of the present paper is to describe the synthesis and structure of some non-stoichiometric Bi–Ti pyrochlores formed initially as impurities during studies of the $Bi_{4-x}Ln_xTi_3O_{12}$ Aurivillius oxides. These have been identified as having the stoichiometry $Bi_{2/3}Ln_{4/3}Ti_2O_7$ when *Ln* is Sm^{3+} or smaller. Single phase samples of pyrochlores with this stoichiometry could not be obtained for the larger lanthanides.

2. Experimental

Five Bi–Ti–*Ln* (where *Ln* = La, Nd, Eu, Ho and Yb) pyrochlores were prepared by the solid state reaction of stoichiometric quantities of Bi_2O_3, TiO_2 and Ln_2O_3. The mixed precursors were pre-heated at 700 °C for 24 hours before firing at 900, 1000 and 1100 °C for durations of 48 hours each. The reaction was monitored by laboratory X-ray diffraction using Cu$K\alpha$ radiation on a Shimadzu D-6000 Diffractometer and showed well formed pyrochlores for Ln^{3+} = Eu, Ho and Yb. Further heating of the Ln^{3+} = La and Nd samples up to 1300 °C at 50 °C intervals for durations of 48 hours each showed possible decomposition. The synchrotron X-ray diffraction data were collected using the MYTHEN microstrip detector on the powder diffractometer at BL-10 of the Australian Synchrotron, Melbourne Australia [14]. The samples were housed in 0.3 mm diameter capillaries that were rotated during the measurements. Data were recorded at room temperature in the angular range $5^\circ < 2\theta < 85^\circ$, using X-rays of wavelength 0.79723 Å as estimated using NIST LaB_6. Neutron powder diffraction data of the samples were measured at room temperature using the high resolution powder diffractometer Echidna at ANSTO's OPAL facility at Lucas Heights [15]. For these measurements the sample was contained in a cylindrical vanadium can. The structures were refined using the program RIETICA [16].

3. Results and discussion

During an attempted synthesis of $Bi_3HoTi_3O_{12}$ the sample was overheated and X-ray analysis of the product revealed it to be a mixture of a pyrochlore and rutile. Analytical microscopy indicated the pyrochlore to have a Bi:Ho:Ti ratio of 1:2:3 or $Bi_{2/3}Ho_{4/3}Ti_2O_7$. Further studies of the Aurivillius oxide series $Bi_2Ln_2Ti_3O_{12}$ also yielded a proportion of their respective pyrochlore of composition $Bi_{2/3}Ln_{4/3}Ti_2O_7$. For $Ln = La^{3+}$ the major product formed was the La doped Aurivillius oxide $Bi_{4-x}La_xTi_3O_{12}$. The relative stability of the Aurivillius phase (as gauged by the growth of the pyrochlore phase in synchrotron X-ray diffraction patterns from "$Bi_2Ln_2Ti_3O_{12}$" prepared using an identical heating regime to that described in the experimental section but with the appropriate Bi:*Ln*:Ti ratio), evident by both inspection of the diffraction data, Fig. 1 and Rietveld analysis, Table 1 decreased as the size of the *Ln* cation decreased from 1.160 Å for $Ln = La^{3+}$ to 1.08 Å for $Ln = Sm^{3+}$. After this size the pyrochlore and Aurivillius oxide co-existed as the pyrochlore became the major phase.

Subsequently we prepared a single phase pyrochlore sample with the composition $Bi_{2/3}Ho_{4/3}Ti_2O_7$, using the appropriate stoichiometric ratio of reagents. Given the ease with which it was formed we sought to use identical conditions to make the analogous oxides with other lanthanides La, Nd, Eu and Yb. As noted in the experimental section of these only *Ln* = Ho, Eu and Yb yielded in single phase samples.

Having established, using analytical microscopy, that the stoichiometry of the single phase pyrochlores were $Bi_{2/3}Ln_{4/3}Ti_2O_7$ we next sought to determine the precise structure of these. The synchrotron X-ray diffraction pattern of $Bi_{2/3}Ho_{4/3}Ti_2O_7$ was well fitted to a conventional pyrochlore model where the Bi and Ho were statistically distributed over the 16*d* sites at $(\frac{111}{222})$ of the cubic space group $Fd\bar{3}m$ (using origin choice 2). In these refinements the Bi:Ho ratio was fixed at 1:2, as determined using analytical microscopy. Whilst generally satisfactory, the displacement parameters for the Bi/Ho cations were larger than those of the other ions and a number of discrepancies were evident at low *d*-values, see Fig. 2. Disorder of the Bi/Ho onto a 96*h* site at (0 *y* −*y*) eliminated these problems and resulted in a marginal improvement in the various *R*-factors, from $R_p = 2.13$, $R_{wp} = 3.27$ and $\chi^2 = 13.56$ to 2.06%, 3.17% and 13.07%, respectively. This model is identical to that found for BZN [11,17] and proved equally successful for samples with Ln^{3+} = Eu and Yb. Whilst most obvious in Bi containing pyrochlores, disorder of the A-type cations has also been observed for other pyrochlores, most noticeably $La_2Zr_2O_7$ [18]. As observed [19] in the stannate pyrochlores $Ln_2Sn_2O_7$, the lattice parameter and Ti-O-Ti angle both decreased as the size of the lanthanide cation was decreased, Table 2.

The existence of cation disorder in these oxides was verified using electron diffraction [20–23]. Transverse polarised diffuse streaking running along the [220]* and [2,−2,0]* directions of reciprocal space is evident in Fig. 3a, while in Fig. 3b the transverse polarised diffuse streaking is seen to be running along the [222]*, [2,2,−2]* and [002]* directions of reciprocal space. In each case the diffuse streaking runs perpendicular to one or other

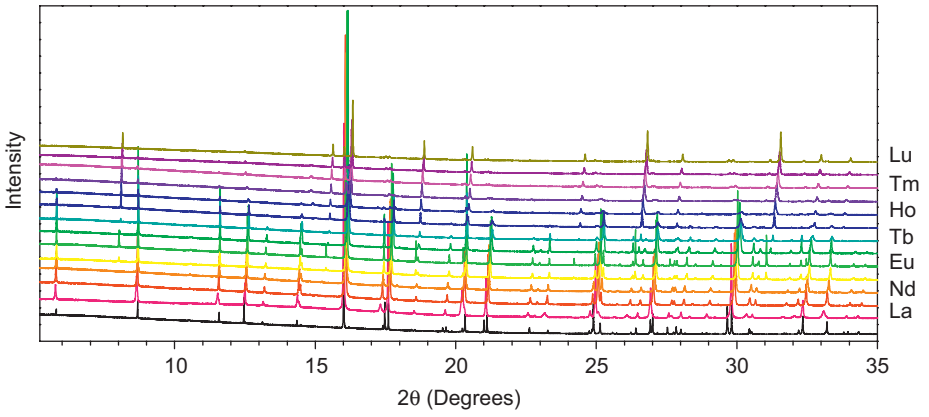

Fig. 1. Diffraction patterns, collected with $\lambda = 0.79723$ Å for samples of nominal composition $Bi_2Ln_2Ti_3O_{12}$ showing the gradual growth of the pyrochlore phase with decreasing cation size. The bottom profile represents $Bi_4Ti_3O_{12}$, and the top profile represents "$Bi_2Lu_2Ti_3O_{12}$", that was identified to be 63.8(3) mole % of the pyrochlore $Bi_{2/3}Lu_{4/3}Ti_2O_7$. All the *Ln* doped samples were synthesised under the same reaction conditions. The Ce and Pm compounds were not prepared.

Table 1
Phase analysis and lattice parameters for the oxides prepared from the reaction of Bi_2O_3+Ln_2O_3+4TiO_2.

Nominal sample	Actual composition	Molar (%)	Weight (%)	Lattice parameters (Å)			Volume (Å^3)	R_p (%)
				a	*b*	*c*		
$Bi_2La_2Ti_3O_{12}$	$Bi_2La_2Ti_3O_{12}$			3.82618(2)		32.9651(3)	482.597(5)	2.51
$Bi_2Pr_2Ti_3O_{12}$	$Bi_2Pr_2Ti_3O_{12}$			3.81199(2)		32.8374(2)	477.169(5)	2.67
$Bi_2Nd_2Ti_3O_{12}$	$Bi_2Nd_2Ti_3O_{12}$			3.80811(1)		32.7852(2)	475.441(4)	2.20
$Bi_2Sm_2Ti_3O_{12}$	$Bi_{2/3}Sm_{4/3}Ti_2O_7$	1.30(2)	9.1(1)	10.2514(1)			1077.33(2)	2.47
	$Bi_2Sm_2Ti_3O_{12}$	99(1)	91(1)	3.79927(2)		32.7353(2)	472.517(5)	
$Bi_2Eu_2Ti_3O_{12}$	$Bi_{2/3}Eu_{4/3}Ti_2O_7$	3.28(5)	20.6(3)	10.24839(4)			1076.383(8)	2.48
	$Bi_2Eu_2Ti_3O_{12}$	97(1)	79(1)	3.79855(2)		32.7318(1)	472.287(4)	
$Bi_2Gd_2Ti_3O_{12}$	$Bi_{2/3}Gd_{4/3}Ti_2O_7$	0.60(3)	4.4(2)	10.2013(2)			1061.61(3)	3.30
	$Bi_2Gd_2Ti_3O_{12}$	99(2)	96(2)	3.78831(3)		32.7104(2)	469.436(6)	
$Bi_2Tb_2Ti_3O_{12}$	$Bi_{2/3}Tb_{4/3}Ti_2O_7$	2.30(8)	15.3(5)	10.1765(1)			1053.88(2)	2.51
	$Bi_2Tb_2Ti_3O_{12}$	98(2)	85(1)	3.78257(5)		32.7084(4)	467.99(1)	
$Bi_2Dy_2Ti_3O_{12}$	$Bi_{2/3}Dy_{4/3}Ti_2O_7$	7.22(8)	37.4(4)	10.16050(5)			1048.93(1)	1.58
	$Bi_2Dy_2Ti_3O_{12}$	93(1)	62.6(6)	3.78246(3)		32.7098(3)	467.978(6)	
$Bi_2Ho_2Ti_3O_{12}$	$Bi_{2/3}Ho_{4/3}Ti_2O_7$	31.3(1)	63.2(2)	10.14783(7)			1045.01(1)	1.48
	$Bi_2Ho_2Ti_3O_{12}$	64.0(4)	33.7(2)	5.3822(1)	5.3371(1)	32.7318(6)	940.23(3)	
	Bi_2O_3	4.72(9)	3.09(6)	5.5214(1)			168.322(7)	
$Bi_2Er_2Ti_3O_{12}$	$Bi_{2/3}Er_{4/3}Ti_2O_7$	44.5(3)	75.5(5)	10.13265(5)			1040.327(9)	1.41
	$Bi_2Er_2Ti_3O_{12}$	55.5(5)	24.5(2)	5.3971(1)	5.3651(1)	32.7928(7)	949.55(3)	
$Bi_2Tm_2Ti_3O_{12}$	$Bi_{2/3}Tm_{4/3}Ti_2O_7$	52.4(3)	80.9(4)	10.11890(4)			1036.095(7)	1.16
	$Bi_2Tm_2Ti_3O_{12}$	47.6(4)	19.1(1)	5.41774(8)	5.38238(8)	32.8125(5)	956.82(2)	
$Bi_2Yb_2Ti_3O_{12}$	$Bi_{2/3}Yb_{4/3}Ti_2O_7$	57.6(3)	84.0(4)	10.10173(3)			1030.830(5)	1.17
	$Bi_2Yb_2Ti_3O_{12}$	42.4(3)	16.0(1)	5.42787(8)	5.39154(8)	32.8257(5)	960.63(2)	
$Bi_2Lu_2Ti_3O_{12}$	$Bi_{2/3}Lu_{4/3}Ti_2O_7$	63.8(3)	87.2(4)	10.08919(3)			1026.997(5)	1.36
	$Bi_2Lu_2Ti_3O_{12}$	36.2(3)	12.8(1)	5.43446(7)	5.39733(7)	32.8274(5)	962.88(2)	

Only for the largest *Ln* cations (La, Pr and Nd) were single phase Aurivillius type oxides formed. All other samples were a mixture of the Aurivillius and pyrochlore oxides.

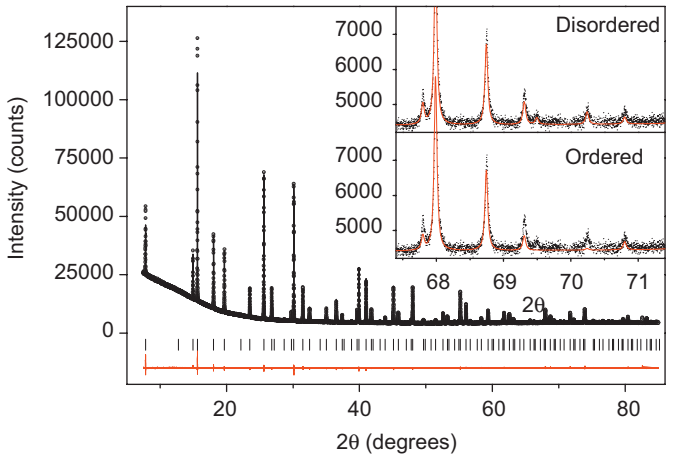

Fig. 2. Observed, calculated and difference profiles for $Bi_{2/3}Ho_{4/3}Ti_2O_7$ prepared from Bi_2O_3+2Ho_2O_3+6TiO_2 recorded using synchrotron X-rays with $\lambda = 0.79723$ Å. The inserts illustrate the improvement in the fit when the Bi and Ho are displaced onto the 96*h* sites.

of the six ⟨110⟩ directions of real space i.e. the observed diffuse takes the form of transverse polarised {110}* sheets of diffuse intensity perpendicular to each of the six ⟨110⟩ directions of real space. The presence of a diffuse distribution of this type requires the existence of β-cristobalite-like orientational disorder of the O′($Bi_{2/3}Ho_{4/3}$) tetrahedral sub-structure shown in Fig. 3c. For further details, see e.g. Zhou et al. [24], Tabira et al. [18], and Withers [22].

The fits to the synchrotron patterns for the three samples studied were excellent, however the precision in the refined oxygen position parameters reflected the impact of the very heavy Bi and *Ln* cations in the structure. To minimise this impact a high resolution neutron diffraction pattern was recorded for the sample of $Bi_{2/3}Yb_{4/3}Ti_2O_7$ (Fig. 4). Refinement of the structure using the disordered model gave $x = 0.3262(1)$. There was no evidence from the Rietveld analysis for any oxygen vacancies. The derived bond distances for this sample are tabulated in Table 2. Comparison of the bond distances obtained from synchrotron X-ray diffraction and neutron diffraction in Table 2 demonstrates the accuracy of the refined structural model.

Finally it is interesting to note the $Bi_{2/3}Ho_{4/3}Ti_2O_7$ composition is analogous to that seen recently in $Bi_{4/3}Na_{2/3}Nb_{4/3}Cr_{2/3}O_{7-d}$ [25] that formed during an attempted synthesis of a perovskite phase.

Table 2
Unit cell, positional and displacement parameters for $Bi_{2/3}Ln_{4/3}Ti_2O_7$ in the cubic space group $Fd\bar{3}m$ from synchrotron X-ray diffraction data. The samples were prepared using the reaction Bi_2O_3+2Ln_2O_3+6TiO_2.

	Eu	Ho	Yb	Yb (neutron)
a (Å)	10.25373(1)	10.18701(1)	10.14530(1)	10.14548(9)
R_p (%)	1.84	2.06	2.11	6.34
R_{wp} (%)	2.98	3.17	3.25	8.05
GOF	14.72	13.04	15.91	2.67
Bi 96*h* 0 *y* −*y*				
y	0.2346(1)	0.2366(1)	0.2359(1)	0.2325(3)
B_{iso} (Å^2)	0.87(1)	0.42(2)	0.11(2)	0.62(4)
Ti 16*c* 0 0 0				
B_{iso} (Å^2)	−0.02(1)	0.14(1)	0.07(2)	0.87(5)
O1 48*f* *x* 1/8 1/8				
x	0.3231(1)	0.3263(2)	0.3276(2)	0.3262(1)
B_{iso} (Å^2)	0.65(3)	0.55(5)	0.65(6)	1.09(2)
O2 8*b* 3/8 3/8 3/8				
B_{iso} (Å^2)	0.93(7)	−0.12(8)	0.47(10)	0.90(4)
Bi–O(1) (Å)	2.574(1)	2.532(2)	2.513(2)	2.517(3)
	2.757(1)	2.690(2)	2.680(2)	2.682(1)
	2.377(1)	2.362(2)	2.335(2)	2.350(1)
Bi–O(2) (Å)	2.2312(8)	2.2139(12)	2.2059(9)	2.205(4)
Ti–O(1) (Å)	1.9615(6)	1.9616(10)	1.9588(9)	1.9535(5)
Ti–O(1)–Ti (°)	135.07(9)	133.28(13)	132.58(12)	133.38(7)

The occupancy of the 96*h* site has been constrained to the appropriate stoichiometry. Selected bond lengths and angles are also given. The negative displacement parameters observed in X-ray diffraction studies reflect the effect of absorption. The results obtained using neutron diffraction for $Bi_{2/3}Yb_{4/3}Ti_2O_7$ are also given.

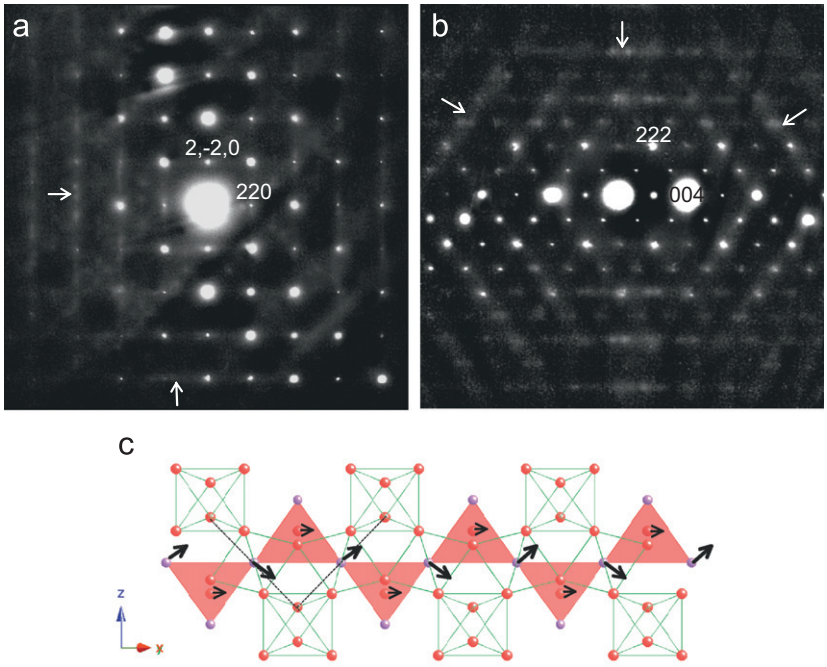

Fig. 3. (a) close to ⟨001⟩ and (b) close to ⟨110⟩ zone axis electron diffraction patterns for $Bi_{2/3}Ho_{4/3}Ti_2O_7$ illustrate the presence of transverse polarised diffuse streaking characteristic of β-cristobalite-like orientational disorder of the O′($Bi_{2/3}Ho_{4/3}$) tetrahedral sub-structure shown in c.

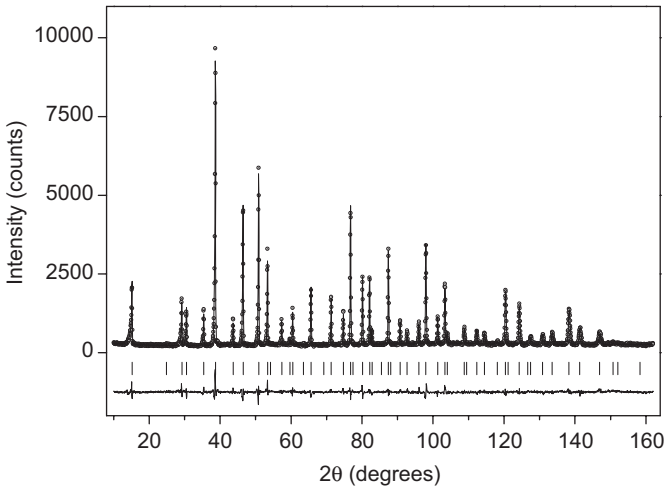

Fig. 4. Neutron powder diffraction Rietveld profiles for $Bi_{2/3}Yb_{4/3}Ti_2O_7$ at room temperature. The format is the same as in Fig. 2.

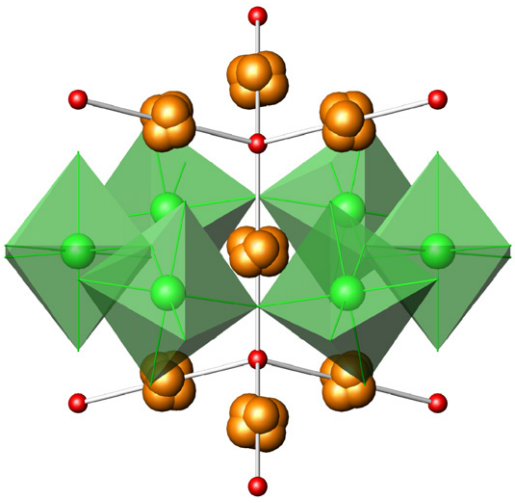

Fig. 5. Representation of the structure of $Bi_{2/3}Ho_{4/3}Ti_2O_7$ highlighting the six-fold disorder of the A-site cations at the centre of hexagonal holes along the ⟨111⟩ direction of the Ti_2O_6 sublattice.

In both pyrochlores the Bi is within the hexagonal holes of the B_2O_6 sublattice but it is displaced away from the 16*c* site that is at the centre of the holes. The off centre displacement is to one of the six equivalent sites as illustrated in Fig. 5. The presence of well structured diffuse rods in the electron diffraction patterns shows this displacement is not random but rather the displacements are coupled with each other. We suggest that in any one moiety the Bi are ordered in 1/3 of occupied 96*h* sites and *Ln* in the remaining 2/3. We see no evidence in the diffraction data to suggest long range ordering of the Bi and Ho cations, indeed the content of unit cell precludes this, suggesting that this ordering occurs on a local scale. Nevertheless the observation of six-fold disorder goes some way to explaining the presence of discrete phases such as the present $Bi_{2/3}Ln_{4/3}Ti_2O_7$ oxides and the previously characterised oxide $Bi_{4/3}Na_{2/3}Nb_{4/3}Cr_{2/3}O_{7-d}$. This disorder results in two long (~2.7 Å) Bi–O bond distances within the hexagonal holes and it is reasonable to suppose that the Bi^{3+} $6s^2$ lone pair electrons are orientated towards these. Just as Bi^{3+} is too large (1.170 Å) to occupy the 16*d* sites in $Bi_2Ti_2O_7$ so too are the lanthanides with $r_{Ln} > 1.08$ Å.

The present work suggests a mechanism to increase the Bi content in the Ti pyrochlores is to increase the size of the hexagonal hole by partially replacing the Ti with a larger cation. Conversely, pyrochlore formation in the Bi–Ti Aurivillius phases may be minimised by doping with larger lanthanides, or by doping Ti with a smaller cation. The challenge now is to use this information to prepare new Bi containing pyrochlores to optimise their physical properties [26].

Acknowledgements

The authors gratefully acknowledge the support of this work from the Australian Research Council. The authors also gratefully acknowledge Dr. Kia Wallwork for assistance at the Australian Synchrotron.

References

[1] I. Radosavljevic, J.S.O. Evans, A.W. Sleight, Journal of Solid State Chemistry 136 (1998) 63.
[2] V. Kahlenberg, H. Bohm, Journal of Alloys and Compounds 223 (1995) 142.
[3] A.L. Hector, S.B. Wiggin, Journal of Solid State Chemistry 177 (2004) 139.
[4] J. Cagnon, D.S. Boesch, N.H. Finstrom, S.Z. Nergiz, S.P. Keane, S. Stemmer, Journal of Applied Physics 102 (2007) 5.
[5] M.A. Subramanian, G. Aravamudan, G.V.S. Rao, Progress in Solid State Chemistry 15 (1983) 55.
[6] T. Watanabe, T. Kojima, T. Sakai, H. Funakubo, M. Osada, Y. Noguchi, M. Miyayama, Journal of Applied Physics 92 (2002) 1518.
[7] B.H. Park, B.S. Kang, S.D. Bu, T.W. Noh, J. Lee, W. Jo, Nature 401 (1999) 682.
[8] Y.Y. Wu, J. Yu, D.M. Zhang, C.D. Zheng, B. Yang, Y.B. Wang, in: Effect of bismuth excess on the crystallization of $Bi_{3.25}La_{0.75}Ti_3O_{12}$ ceramic and thin film, Taylor & Francis, London, 2008, p. 11.
[9] Y.Y. Wu, D.M. Zhang, J. Yu, Y.B. Wang, Materials Science and Engineering B—Advanced Functional Solid-State Materials 149 (2008) 34.
[10] J.C. Nino, M.T. Lanagan, C.A. Randall, Journal of Applied Physics 89 (2001) 4512.
[11] B. Melot, E. Rodriguez, T. Proffen, M.A. Hayward, R. Seshadri, Materials Research Bulletin 41 (2006) 961.
[12] C.E. Bamberger, H.W. Dunn, G.M. Begun, S.A. Landry, Journal of Solid State Chemistry 58 (1985) 114.
[13] A. Garbout, S. Bouattour, A.W. Kolsi, Journal of Crystal Growth 307 (2007) 219.
[14] K.S. Wallwork, B.J. Kennedy, D. Wang, AIP Conference Proceedings 879 (2007) 879.
[15] K.D. Liss, B. Hunter, M. Hagen, T. Noakes, S. Kennedy, Physica B—Condensed Matter 385–386 (2006) 1010.
[16] B.A. Hunter, C.J. Howard, A Computer Program for Rietveld Analysis of X-Ray and Neutron Powder Diffraction Patterns, Lucas Heights Research Laboratories, Sydney, 1998, p. 1.
[17] T.A. Vanderah, I. Levin, M.W. Lufaso, European Journal of Inorganic Chemistry (2005) 2895.
[18] Y. Tabira, R.L. Withers, T. Yamada, N. Ishizawa, Zeitschrift für Kristallographie 216 (2001) 92.
[19] B.J. Kennedy, B.A. Hunter, C.J. Howard, Journal of Solid State Chemistry 130 (1997) 58.
[20] B. Nguyen, Y.R. Liu, R.L. Withers, Journal of Solid State Chemistry 180 (2007) 549.
[21] H.B. Nguyen, L. Noren, Y. Liu, R.L. Withers, X.Y. Wei, M.M. Elcombe, Journal of Solid State Chemistry 180 (2007) 2558.
[22] R.L. Withers, Zeitschrift Fur Kristallographie 220 (2005) 1027.
[23] R.L. Withers, T.R. Welberry, A.K. Larsson, Y. Liu, L. Noren, H. Rundlof, F.J. Brink, Journal of Solid State Chemistry 177 (2004) 231.
[24] Q.D. Zhou, B.J. Kennedy, V. Ting, R.L. Withers, Journal of Solid State Chemistry 178 (2005) 1575.
[25] G.J. Thorogood, B.J. Kennedy, Ismunadar, M. Avdeev, T. Kamiyama, Journal of Physics and Chemistry of Solids 69 (2008) 918.
[26] Y. Hou, Z.M. Huang, J.Q. Xue, Y.N. Wu, X.M. Shen, J.H. Chu, Applied Physics Letters 86 (2005) 3.